Cooperative Binding and Chirogenesis in an Expanded Perylene Bisimide Cyclophane

Divya P. Sukumaran,[†] Kazutaka Shoyama,[†‡] Rajeev K. Dubey,[†] and Frank Würthner[†‡]*

[†]Institut für Organische Chemie, Universität Würzburg, Am Hubland, 97074 Würzburg, Germany
[‡]Center for Nanosystems Chemistry (CNC), Universität Würzburg, 97074 Würzburg, Germany

KEYWORDS. Cyclophane, Host–guest interactions, Cooperativity, Charge-transfer, Chirality

---

ABSTRACT: Encapsulation of more than one guest molecule into a synthetic cavity is a highly desirable, yet a highly challenging task to achieve for neutral supramolecular hosts in organic media. Herein, we report a neutral perylene bisimide (PBI) cyclophane, which has a tailored chiral cavity with interchromophoric distance of 11.2 Å, capable of binding two aromatic guests in a π-stacked fashion. Detailed host–guest binding studies with a series of aromatic guests revealed that the encapsulation of the second guest in this cyclophane is notably more favored than the first one. Accordingly, for the encapsulation of coronene dimer, cooperativity factor (α) as high as 485 was observed, which is unexpectedly high for neutral host–guest systems. Further, a successful chirality transfer, from the chiral host to encapsulated coronenes, resulted in a chiral charge-transfer (CT) complex and the rare observation of circularly polarized emission originating from the CT state for a non-covalent donor–acceptor assembly in solution. The involvement of the CT state also afforded an enhancement in the luminescence dissymmetry factor (g_{lum}) value due to its relatively large magnetic transition dipole moment. The 1:2 binding pattern and chirality-transfer were unambiguously verified by single crystal X-ray diffraction analysis of the host–guest superstructures.

Introduction

Supramolecular hosts have the intriguing ability to provide highly selective and structure specific interactions at the molecular level.[1-2] Therefore, several classes of synthetic host molecules, including cavitands,[3-4] cyclophanes,[5-7] and macrocycles,[7-11] as well as cages,[12-15] clefts,[16] tweezers,[17] and π-receptors,[18-20] have been reported since the period when Lehn, Cram and Pedersen were recognized for their pioneering receptor design for molecular recognition of cations. The focus of the host–guest studies involving these hosts has been on the optimization of the parameters governing the strength of binding of one guest molecule.[21-23] Resultantly, numerous studies have found strategies for establishing systems with ultra-high binding energies, which could even span to attomolar affinity of guests to supramolecular hosts in 1:1 stoichiometry.[24]

Among the enormous number of examples available in literature for molecular recognition, host–guest recognition in 1:1 stoichiometry predominates in contrast to the examples of multiple guest binding that we see in the biological world.[25] Binding of multiple guests inside an artificial cavity is highly desirable as it has the potential to enable new modes of interactions between the guest molecules. This can lead to the emergence of collective ensemble properties which could be utilized for exploiting the functionality of these supramolecular architectures in several fields like catalysis.[26-27] However, designing cavities which could bind more than one guest is challenging as the system has to compensate for the entropy loss, which makes the process more energetically demanding. Therefore, one or more strong interactions (e.g., electrostatic attraction) between the host and guest molecules are essential to drive the process. In this regard, so far, the metal-organic cages are the prime example, wherein the charged metal ions may attract and bind oppositely charged guests making the multiple guest binding feasible. Further, these water-soluble cages take the advantage of strong hydrophobic effects to enforce the simultaneous binding of hydrophobic guests in aqueous media as previously been achieved by Yoshizawa, Fujita, and others.[28-30]

In contrary, there are only few artificial supramolecular hosts, other than the metal-organic cages, that can encapsulate more than one guest and can demonstrate high degree of positive cooperativity in guest recognition. For example, among cyclophanes, there is one recent example of diradical dicationic host reported by Stoddart and co-workers that demonstrates the binding of two methyl viologen radical cations taking the advantage of strong radical-pairing interactions.[31] Another positively charged organic cage,[32] also reported by Stoddart and co-workers, shows cooperative binding of pyrene-1-carbaldehyde guest (cooperativity factor, α = 127) by utilizing cation–dipole and dipole–dipole interactions. Also, recently an ether linked molecular tube has been reported showing binding of DABCO based organic cations with high degree of cooperativity in 2:1

stoichiometry (α = 580), which also involves charge repulsion interactions in addition to hydrogen bonding interactions between two host molecules to form a capsule with guest.[33] Another example showing high cooperative binding in literature is from Gong and co-workers of an oligoamide macrocycle (α = 4–5333) that involves a guest-induced stacking of host and takes advantage of ion–dipole interactions in guest binding.[34-35] As far as we know, no reports are available so far with neutral host–guest systems showing high positive cooperative binding.

Herein, we report an inherently chiral perylene bisimide-based cyclophane with remarkably high cooperativity in binding polycyclic aromatic hydrocarbons (PAHs), arising mainly due to the dispersion interactions between the host and the guest. Another important feature of this cavity is that it serves as a template for inducing chirality on achiral guests and, accordingly, its binding with relatively π-electron-rich coronene results in a chiral charge-transfer (CT) complex and a circularly polarized emission from the CT state with an enhanced luminescence dissymmetry factor (g_{lum}) value, benefiting from the relatively large magnetic transition dipole moment in the CT state.[36-37] It is noteworthy that for non-covalent donor–acceptor systems, such intermolecular CT-CPL activity in solution state has only been observed previously in the molecular assemblies, but not in monomeric donor–acceptor-based systems.

Results and discussion

Synthesis and characterization

The large twisted aromatic units and the elongated spacers are the crucial parts in the design of the herein presented cyclophane. The twisted aromatic core of 1,7-bay-bridged perylene bisimide (PBI) provides a large π-surface for dispersion interactions to shape-complementary guests and the bay-bridging unit provides a good solubility to the resultant cyclophane in organic solvents (Figure 1a). For the spacer units, 4,4'-dimethylbiphenyl moiety was chosen as it provides an interchromophoric distance of ca. 11 Å, which is ideal to encapsulate two aromatic guests in the cavity as a π-stack. The synthesis of enantiomerically pure cyclophanes, **cyc-*PP*** and **cyc-*MM*,** was achieved by following our previously reported synthetic route for a chiral PBI cyclophane of smaller cavity size.[38] Accordingly, the desired cyclophanes were obtained by the final cyclization of bay-bridged enantiopure perylene dianhydride (***P*** or ***M)*** with [1,1'-biphenyl]-4,4'-diyldimethanamine under highly dilute conditions following the Ziegler-Ruggli dilution principle (Figure 1a). The cyclophane (**cyc-*PP*** or **cyc-*MM***) was then isolated in a yield of 12% and then fully characterized using NMR spectroscopy, mass spectrometry, and single-crystal X-ray diffraction (XRD) analysis.

The high-resolution MALDI-TOF mass spectrum of the cyclophane unambiguously showed the molecular ion peak (M^+) and the isotopic distributions consistent with its molecular formula (Figure 1b). Similarly, all the crucial proton

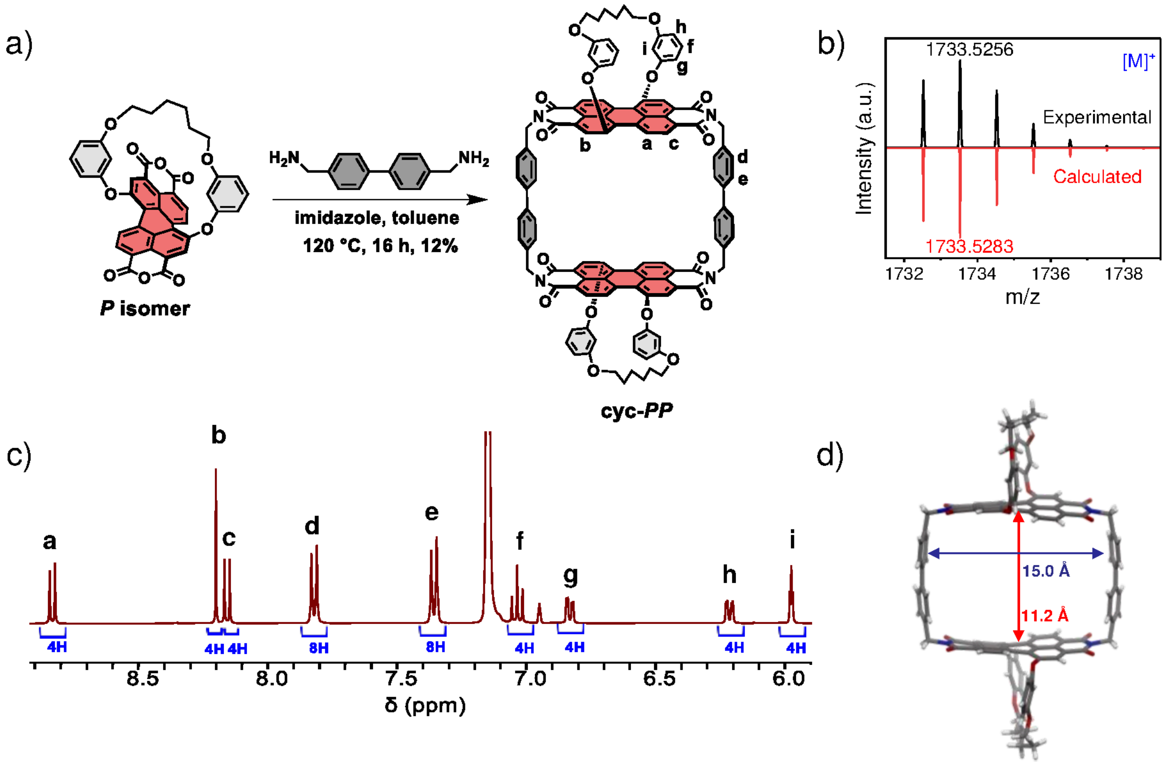

Figure 1. a) Synthesis of *PP*-isomer of the cyclophane (**cyc-*PP***). b) MALDI-TOF MS spectra of **cyc-*PP***. c) Partial 400 MHz ^{1}H NMR spectra of the **cyc-*PP*** showing chemical shifts of aromatic protons in C_6D_6 at 295 K. d) Molecular structure of **cyc-*PP*** obtained by single-crystal X-ray diffraction analysis.

signals could be clearly seen and assigned in the 400 MHz room temperature ^{1}H NMR spectrum of the cyclophane in deuterated benzene. In the aromatic region, the typical two doublets pertaining to the 1,7-substituted PBI core can be seen at 8.84 and 8.16 ppm, and the relevant one singlet at 8.21 ppm (Figure 1c). The two doublets originating from the biphenyl spacer moiety can also be seen at 7.83 and 7.36 ppm. As well as the four signals corresponding to four protons of the bay-bridging phenoxy moieties were observed in the range between 7.07–5.98 ppm. The observation of only one set of well-resolved signals in ^{1}H NMR spectrum at 295 K indicates a highly symmetric structure of the cyclophane.

Host–guest recognition

As observed in the single crystal structure of **cyc-*PP*** (Figure 1d), the interchromophoric distance is 11.2 Å that is around thrice the typical π–π interaction distance and, hence, the cyclophane should be suitable to offer the encapsulation of two aromatic guests as a π-stack supported by π–π interactions. Therefore, the molecular recognition properties of **cyc-*PP*** were investigated with host–guest titration experiments in toluene employing UV/Vis absorption spectroscopy. For these studies, two sets of aromatic guests were investigated, i.e., triphenylene, perylene, and coronene as the planar guests, whereas [4]-helicene and dibenzo[*g*,*p*]chrysene as the non-planar guests.

The spectral changes in the UV/Vis absorption of **cyc-*PP*** upon the addition of coronene are shown in Figure 2a. The intensity of $S_0 \rightarrow S_1$ transitions decreases upon complexation and a new charge-transfer band arises in the higher wavelength region of the spectrum. The fitting of the obtained titration data resulted in a sigmoidal 1:2 fitting curve, which is typical for cooperative binding, with $K_1 = 5.7 \times 10^2\ \mathrm{M^{-1}}$ and a significantly increased $K_2 = 6.9 \times 10^4\ \mathrm{M^{-1}}$, affording a cooperativity factor $\alpha = 485$ (Figure 2b). The high cooperativity in binding is clearly evident in mole fraction ratio plot as well, wherein the mole fraction of the 1:2 complex sharply increases with the addition of guest (Figure 2c).

The binding constants and cooperativity factor for all the guests used for titration studies are summarized in Table 1, with their titration curves and mole fraction ratio plots in the supplementary information (Figures S7–S10). In each series, the binding affinity increased with the increase in the π-surface area of guests involved in host–guest interaction (Figure 2d). Most interestingly, for all the studied guests, the second binding was found to be stronger as compared to the first binding. This can be attributed to the effective guest–guest interaction inside the cavity based on the observation that the cooperativity also increased with the increase of the π-surface of the guests. Thus, for coronene that

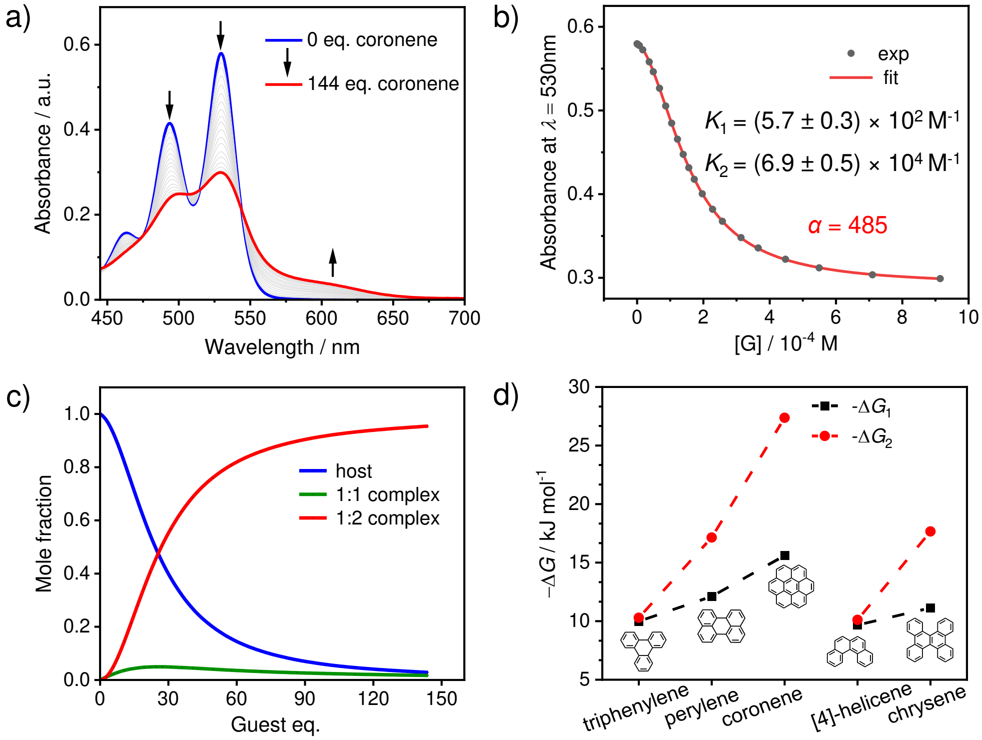

Figure 2. a) Changes in UV/Vis absorption spectrum of **cyc-*PP*** in toluene upon addition of coronene at 22°C (c_{host} = 6 μM). b) The fitting curve plot for absorbance at λ=530 nm with the nonlinear curve fitting with 1:2 host–guest model in Bindfit.[39] The binding constant is the average of two experiments and the error indicated is the calculated standard deviation. c) The mole fraction plot for the titration experiment with coronene as guest. d) Plot of Gibbs free energy calculated at 22 °C for different guests.

Table 1. Binding constants (K_1 and K_2 for first and second binding, respectively) and corresponding Gibbs free energies (ΔG_1 and ΔG_2), and cooperativity factor for 1:2 complexation of cyc-*PP* and aromatic guests at 22 °C in toluene.

Guest	K_1 (M^{-1}) [a]	K_2 (M^{-1}) [a]	$-\Delta G_1$ (kJ mol^{-1}) [b]	$-\Delta G_2$ (kJ mol^{-1}) [b]	Cooperativity factor (α) [c]
Triphenylene	5.8×10^{1}	6.6×10^{1}	9.9	10.2	5
Perylene	1.4×10^{2}	1.1×10^{3}	12.1	17.1	31
Coronene	5.7×10^{2}	6.9×10^{4}	15.5	27.3	485
[4] -Helicene	5.1×10^{1}	6.1×10^{1}	9.6	10.1	5
Dibenzo[*g*,*p*]chrysene	9.3×10^{1}	1.3×10^{3}	11.1	17.6	57

[a]Binding constants are calculated using global fit analysis (490 nm to 540 nm) with Bindfit[39] by fitting of UV/Vis absorption titration data. The reported binding constants are the average of two separate titration analysis and the fitting error was within 0.1 kJ mol^{-1} of error in Gibbs free energy for all cases. [b]Gibbs free energy has been calculated using $\Delta G = -RT \ln K$. [c]Cooperativity factor is given by $\alpha = \frac{4K_2}{K_1}$.

has the largest π-surface, highest cooperativity factor was observed, which is unusually high for a neutral host–guest system in which stronger forces, such as ion–dipole, ion–pairing, H-bonding, or radical interactions, are absent.[40-41] Such a high cooperativity can be rationalized by the fact that the large empty cavity, which is less preorganized, can only weakly bind the first guest molecule with the aid of π–π interaction between host and guest. Whereas during the second binding event, the cavity is more adapted with smaller cavitation volume for guest binding offering additional π–π interaction between two guest molecules in addition to the host–guest interaction. This notion is further supported by the observation that the cooperativity factor is related to the aromatic π-surface of the guest molecules encapsulated. It increases from the smaller triphenylene to the larger coronene among the planar PAHs (Figure 2d). For the non-planar guests as well, while both the first and second binding were significantly less efficient as compared to the planar guests, the cooperativity factor increased with the increase of π-surface of the guest molecules.

The high cooperativity involved in binding of coronene was further elucidated with the help of high-resolution mass spectrometry, wherein the molecular ion peak corresponding to the 1:2 host–guest complex was observed, but not the one corresponding to 1:1 complex (Figure S6). The co-crystals formed by the cyclophane with guest molecules also provided proof for the encapsulation of two guest molecules inside the cyclophane cavity (Figure 3). Further, the co-crystal of perylene molecules inside **cyc-*PP*** unambiguously depicted the chirality transfer of the host to the two guest molecules inside its cavity wherein the twist of the guest *π*-core is clearly evident with a twist angle of 6.85°. Whereas, in the co-crystals with coronene as guest, the core twist is relatively less evident with a smaller twist angle of 2.52° because of the more rigid core of coronene.

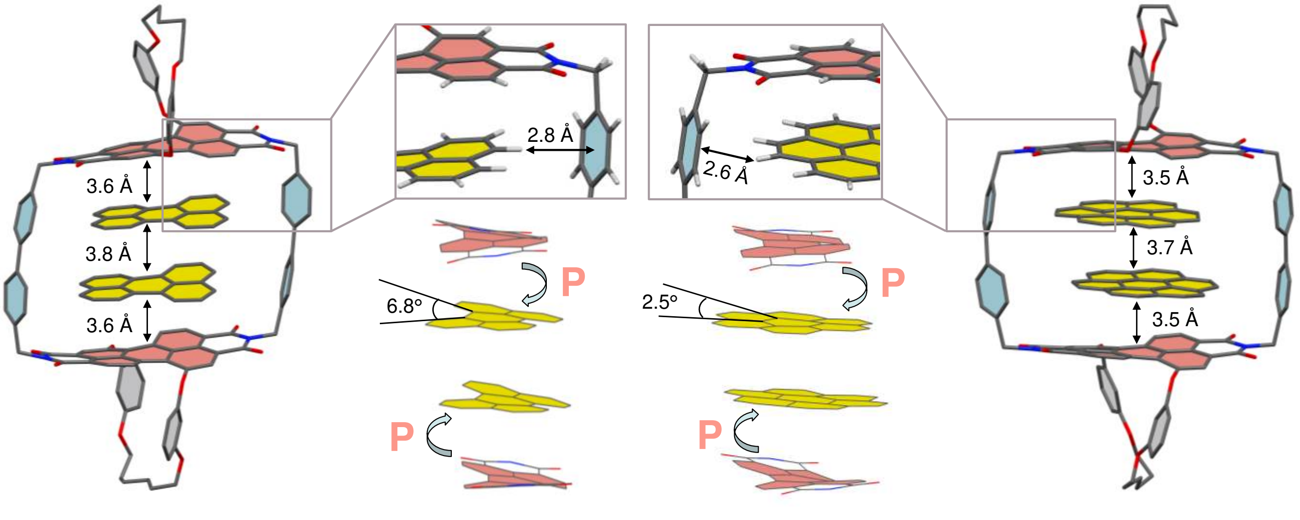

Figure 3. Single crystal structure of (perylene)$_2\subset$**cyc-*PP*** (left) and (coronene)$_2\subset$**cyc-*PP*** (right), and the depiction of C-H⋯π interactions and chirality transfer from the host to the guests. Notes: solvent molecules and hydrogen atoms are omitted for clarity. In the inset images, hydrogen atoms are displayed for showing the C-H⋯π interactions involved between the aromatic ring of the spacer and the guest protons. To visualize the chirality transfer, π-surfaces of the host and guests are shown. The twist angles of the guests are measured between the planes containing each naphthalene subunit.

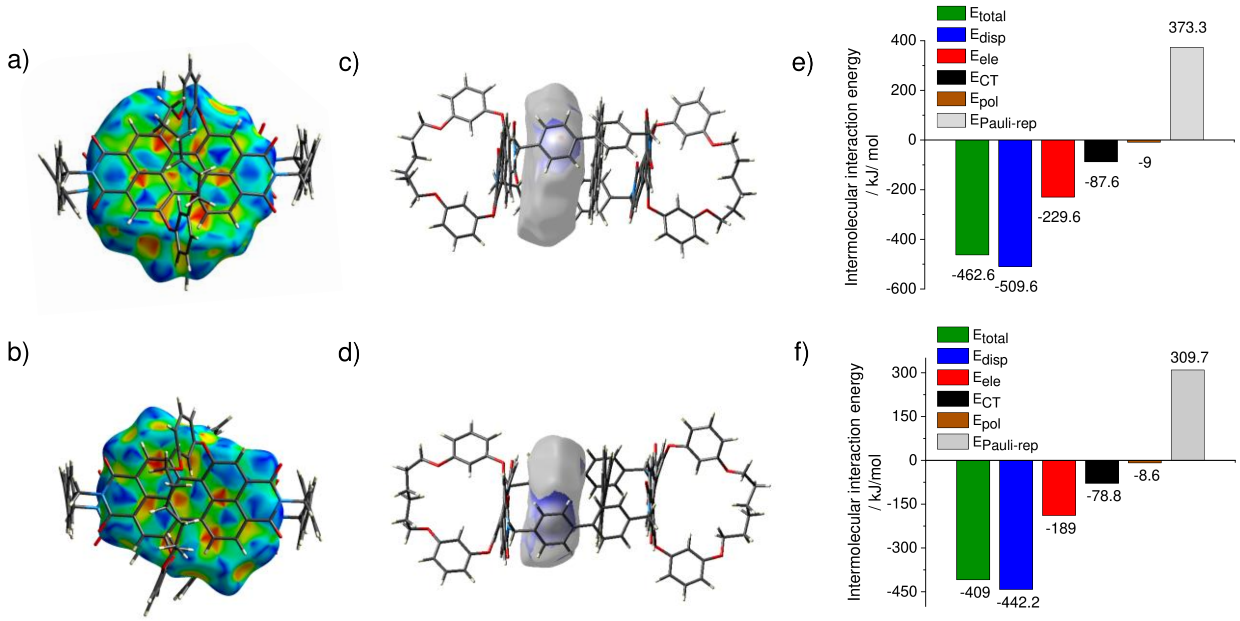

Figure 4. Hirshfeld surface plotted over shape index of guest with view from top showing the π–π interactions between PBI plane of **cyc-*PP*** and a) coronene in (coronene)$_2$⊂**cyc-*PP***, b) perylene in (perylene)$_2$⊂**cyc-*PP***. Hirshfeld d_{norm} surfaces for the guest indicating the involved C-H⋯π interaction in c) (coronene)$_2$⊂**cyc-*PP***, d) (perylene)$_2$⊂**cyc-*PP***. Interacting area of the surface is highlighted with blue colour. ALMO energy decomposition analysis performed on X-ray crystal structures of e) (coronene)$_2$⊂**cyc-*PP***, f) (perylene)$_2$⊂**cyc-*PP***.

The distance between the aromatic surfaces (measured from the centroids of central π-ring), i.e., 3.5–3.8 Å, establishes the π–π interaction involved between the aromatic planes as the driving force for complexation. However, in addition to the π–π interactions, C-H⋯π interactions,[42] between the protons of guest and aromatic rings of the spacer unit, contribute to the guest binding in view of the short distance of 2.6–3.1 Å for (perylene)$_2$⊂**cyc-*PP*** and (coronene)$_2$⊂**cyc-*PP*** (Figure 3).

In order to get an exact information and magnitude of the non-covalent forces involved in the host–guest superstructures, Hirshfeld surface analysis[43] and ALMO energy decomposition analysis were carried out using the corresponding X-ray crystal structures of (perylene)$_2$⊂**cyc-*PP*** and (coronene)$_2$⊂**cyc-*PP***. The Hirshfeld surface analysis clearly showed the adjacent red and blue triangles on the shape index mapping of guest (Figures 4a–b, and S19), which confirmed the presence of π–π interactions between host–guest and guest–guest surfaces. It also revealed the involvement of C-H⋯π interaction surfaces, highlighted by blue color, in the complexation (Figure 4c–d). Finally, the ALMO energy decomposition analysis confirmed that the complexation of host is predominantly due to dispersion interactions between the adjacent π-surfaces for both coronene and perylene (Figures 4e–f). While C-H⋯π interactions, which are electrostatic in character, have a significantly lower contribution in the total energy. Quite surprisingly, the contribution of charge-transfer interactions remained much smaller even for the electron-rich coronene that shows the formation of a pronounced charge-transfer band upon complexation with the electron-deficient host (Figure 2a).

Chirogenesis

In (coronene)$_2$⊂**cyc-*PP*** complex, the donor–acceptor interaction exists between the electron-rich coronene and electron-deficient cyclophane as evident from the emergence of a new charge-transfer (CT) band in the absorption spectrum of the corresponding host–guest complex and ALMO-EDA analysis (Figure 2a and 4e). Thus, following the titration data and chirality transfer observed in XRD structure analysis, chiral spectroscopic measurements were carried out to probe the ground and excited state chirality of the **cyc-*PP*/cyc-*MM*** complex with coronene.

The chiral character of the CT complex was confirmed by the newly formed band at higher wavelengths in the CD spectra, showing a positive signal for (coronene)$_2$⊂**cyc-*PP***

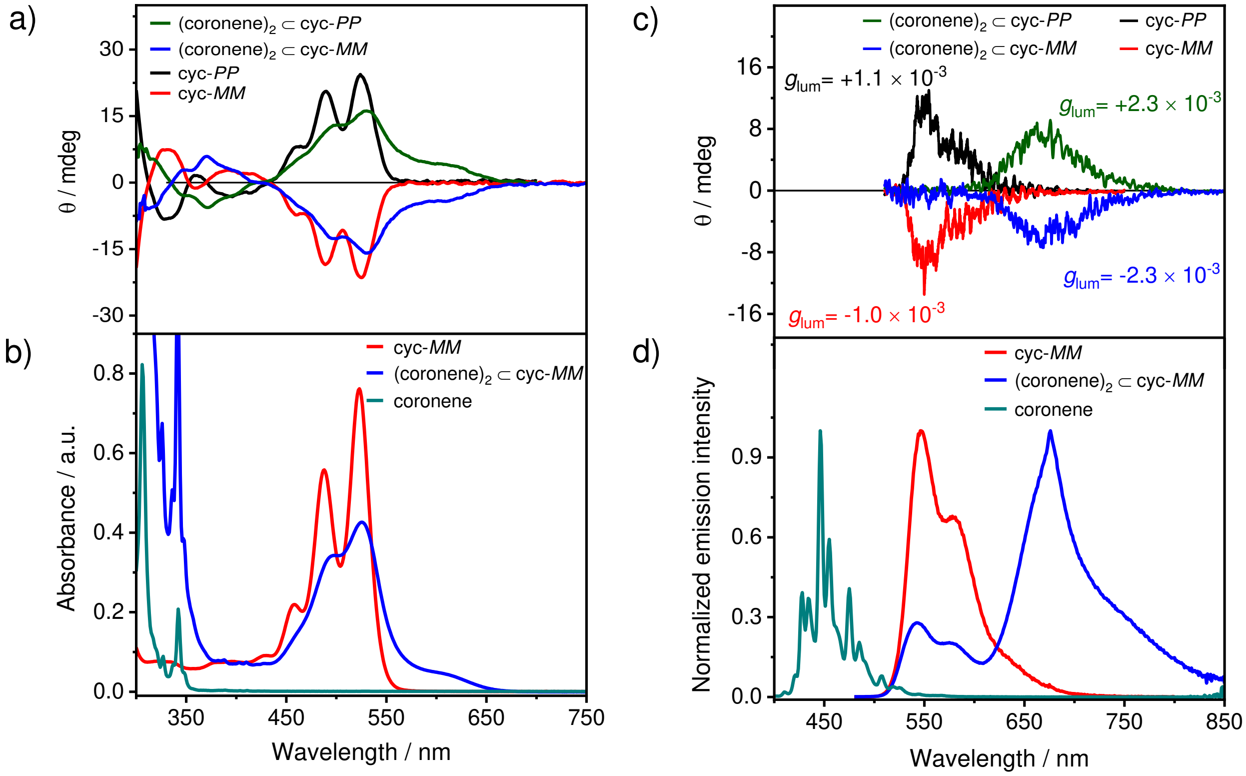

Figure 5. a) CD spectra, b) UV/Vis absorption spectra, c) CPL spectra and d) normalized emission spectra of **cyc-*PP*/cyc-*MM*** without and with coronene (4 equivalents) as guest in CCl_4 at 20 °C (c_{host}=9.5 × 10^{-5} M). Emission and CPL spectra were obtained by exciting at 460 nm. Absorption and emission spectra of free coronene is given as reference (excitation at 342 nm).

complex and a negative signal for (coronene)$_2\subset$**cyc-*MM*** complex (Figure 5a). The addition of coronene to the cyclophane resulted in interesting changes to the emission properties as well. While the PBI emission was quenched due to the charge-transfer interactions, a new CT-emission band was emerged at higher wavelengths (Figure 5d). Accordingly, upon excitation of the host–guest complex at the newly formed charge-transfer absorption band, the corresponding circularly polarized luminescence band was observed at a red-shifted wavelength of 667 nm (Figure 5c). Interestingly, g_{lum} of the host–guest CT complex is enhanced by a factor of two as compared to the chiral host species, from ±1 × 10^{-3} to ±2 × 10^{-3}. This enhancement is significant considering that the chiral emissive organic systems with high g_{lum} values are still challenging to achieve due to inherently suppressed magnetic transition dipole moment ($|\boldsymbol{m}|$) and relatively large electric transition dipole moment ($|\boldsymbol{\mu}|$) of the organic molecules [$g_{lum} \approx 4|\boldsymbol{m}|\cos\theta/|\boldsymbol{\mu}|$].[44-47] Herein, the CPL enhancement for (coronene)$_2\subset$**cyc-*PP*** complex can be rationalized by the involvement of a CT state that has a relatively large magnetic transition dipole moment of the CT complexes due to the presence of unpaired electrons in the CT state, and a small electric transition dipole moment as evident from the weak CT absorption band.[48]

It has to be emphasized that the CPL enhancement by taking advantage of CT interactions is a relatively new approach with the first report in 2019, wherein Liu & Duan et al. achieved an enhanced CPL in emissive CT complexes consisting of chiral electron donor and achiral electron acceptor in solid and gel phase.[49] Thereafter, other donor–acceptor based chiral systems, ranging from supramolecular copolymers to covalently linked macrocyclic architectures, with enhanced CPL have been reported.[50-58] Notably, the systems showing CT-CPL in solution state are scarce as they usually involve emission quenching[59] and there are no reports of non-covalent organic CT host-guest complexes exhibiting CPL activity in the solution state as per our knowledge.

Conclusion

In summary, an expanded cyclophane composed of chiral perylene bisimides was synthesized, and its ability to bind different PAH dimers has been demonstrated with the manifestation of host chirality transfer to the achiral guest molecule. In guest binding, the cyclophane exhibited a strong allosteric cooperativity, which could be directly correlated to the size of the aromatic π-surface of the guest involved in binding. Thus, this study provided a proof that even the weakest intermolecular forces – dispersion interactions – can be manipulated to design systems offering highly cooperative interactions for molecular recognition as in the biological world. As the first binding guarantees the second binding event due to the cooperative nature of guest binding, this class of macrocycles can be easily employed to accomplish the intermolecular interactions between guest molecules inside the cavity, which could be further exploited for achieving the goals like electron/energy transfer between these molecules. Such cavities can also serve as an ideal catalytic platform by increasing the effective concentration of two reacting molecules by bringing them to proximity and can also offer selectivity for those inner-cavity reactions. Finally, with a precise combination of CT interactions and chiral induction, this work demonstrates the manipulation of CT interaction in the non-covalent host–guest systems to achieve enhanced circularly polarized emission, which has been particularly challenging in the field of chiral organic emitters.

ASSOCIATED CONTENT

Data Availability Statement

The data underlying this study is available in the Supporting Information and in Zenodo at https://doi.org/10.5281/zenodo.11651793.

Supplementary information

The Supporting Information is available free of charge at https://pubs.acs.org.

Methods and equipment, synthesis and characterization, titration data, single-crystal X-ray diffraction and analysis, and theoretical calculations

Accession Codes

CCDC 2362260-2362262 contains the supplementary crystallographic data for this paper. These data can be obtained free of charge via www.ccdc.cam.ac.uk/data_request/cif, or by emailing data_request@ccdc.cam.ac.uk, or by contacting The Cambridge Crystallographic Data Centre, 12 Union Road, Cambridge CB2 1EZ, UK; fax: +44 1223 336033.

AUTHOR INFORMATION

Corresponding Author

* Frank Würthner
Institut für Organische Chemie, Universtät Würzburg, 97074, Würzburg, Germany; Center for Nanosystems Chemistry (CNC), Universität Würzburg, 97074, Würzburg, Germany; orcid.org/0000-0001-7245-0471; Email: wuerthner@uni-wuerzburg.de

Author Contributions

Funding Sources

Notes

ACKNOWLEDGEMENT

We acknowledge DESY (Hamburg, Germany), a member of the Helmholtz Association HGF, for providing experimental facilities at PETRA III (proposal No I-20211168 and I-20220338). We thank Dr. Manuel Weh for the scientific discussions and Julius Albert for technical assistance in synthesis.

REFERENCES

1. Schneider, H.-J.; Yatsimirsky, A. K., Selectivity in Supramolecular Host–Guest Complexes. *Chem. Soc. Rev.* **2008,** *37*, 263-277.
2. Huang, F.; Anslyn, E. V., Introduction: Supramolecular Chemistry. *Chem. Rev.* **2015,** *115*, 6999-7000.
3. Pinalli, R.; Suman, M.; Dalcanale, E., Cavitands at Work: From Molecular Recognition to Supramolecular Sensors. *Eur. J. Org. Chem.* **2004,** *2004*, 451-462.
4. Biros, S. M.; Rebek, J. J., Structure and Binding Properties of Water-Soluble Cavitands and Capsules. *Chem. Soc. Rev.* **2007,** *36*, 93-104.
5. Diederich, F., Complexation of Neutral Molecules by Cyclophane Hosts. *Angew. Chem. Int. Ed. Engl.* **1988,** *27*, 362-386.
6. Roy, I.; David, A. H. G.; Das, P. J.; Pe, D. J.; Stoddart, J. F., Fluorescent Cyclophanes and Their Applications. *Chem. Soc. Rev.* **2022,** *51*, 5557-5605.
7. Spenst, P.; Würthner, F., Photo- and Redoxfunctional Cyclophanes, Macrocycles, and Catenanes Based on Aromatic Bisimides. *J. Photochem. Photobiol. C* **2017,** *31*, 114-138.
8. Iyoda, M.; Yamakawa, J.; Rahman, M. J., Conjugated Macrocycles: Concepts and Applications. *Angew. Chem. Int. Ed.* **2011,** *50*, 10522-10553.
9. Liu, Z.; Nalluri, S. K. M.; Stoddart, J. F., Surveying Macrocyclic Chemistry: From Flexible Crown Ethers to Rigid Cyclophanes. *Chem. Soc. Rev.* **2017,** *46*, 2459-2478.
10. Yudin, A. K., Macrocycles: Lessons from the Distant Past, Recent Developments, and Future Directions. *Chem. Sci.* **2015,** *6*, 30-49.
11. Han, X.-N.; Han, Y.; Chen, C.-F., Recent Advances in the Synthesis and Applications of Macrocyclic Arenes. *Chem. Soc. Rev.* **2023,** *52*, 3265-3298.
12. Zhang, G.; Mastalerz, M., Organic Cage Compounds – from Shape-Persistency to Function. *Chem. Soc. Rev.* **2014,** *43*, 1934-1947.
13. Percástegui, E. G.; Ronson, T. K.; Nitschke, J. R., Design and Applications of Water-Soluble Coordination Cages. *Chem. Rev.* **2020,** *120*, 13480-13544.
14. Zhang, D.; Ronson, T. K.; Zou, Y.-Q.; Nitschke, J. R., Metal–Organic Cages for Molecular Separations. *Nat. Rev. Chem.* **2021,** *5*, 168-182.
15. McConnell, A. J., Metallosupramolecular Cages: From Design Principles and Characterisation Techniques to Applications. *Chem. Soc. Rev.* **2022,** *51*, 2957-2971.
16. Rebek Jr, J.; Askew, B.; Islam, N.; Killoran, M.; Nemeth, D.; Wolak, R., Synthetic Receptors: Size and Shape Recognition within a Molecular Cleft. *J. Am. Chem. Soc.* **1985,** *107*, 6736-6738.
17. Hardouin–Lerouge, M.; Hudhomme, P.; Sallé, M., Molecular Clips and Tweezers Hosting Neutral Guests. *Chem. Soc. Rev.* **2011,** *40*, 30-43.
18. Teichmann, B.; Krause, A.-M.; Lin, M.-J.; Würthner, F., Enantioselective Recognition of Helicenes by a Tailored Chiral Benzo[ghi]perylene Trisimide π-Scaffold. *Angew. Chem. Int. Ed.* **2022,** *61*, e202117625.
19. Pigulski, B.; Shoyama, K.; Sun, M.-J.; Würthner, F., Fluorescence Enhancement by Supramolecular Sequestration of a C54-Nanographene Trisimide by Hexabenzocoronene. *J. Am. Chem. Soc.* **2022,** *144*, 5718-5722.
20. Mahl, M.; Niyas, M. A.; Shoyama, K.; Würthner, F., Multilayer Stacks of Polycyclic Aromatic Hydrocarbons. *Nat. Chem.* **2022,** *14*, 457-462.
21. Assaf, K. I.; Nau, W. M., Cucurbiturils: From Synthesis to High-Affinity Binding and Catalysis. *Chem. Soc. Rev.* **2015,** *44*, 394-418.
22. Escobar, L.; Ballester, P., Molecular Recognition in Water Using Macrocyclic Synthetic Receptors. *Chem. Rev.* **2021,** *121*, 2445-2514.
23. Sarkar, S.; Ballester, P.; Spektor, M.; Kataev, E. A., Micromolar Affinity and Higher: Synthetic Host–Guest Complexes with High Stabilities. *Angew. Chem. Int. Ed.* **2023,** *62*, e202214705.
24. Cao, L.P.; Sekutor, M.; Zavalij, P. Y.; Mlinaric-Majerski, K.; Glaser, R.; Isaacs, L., Cucurbit[7]uril. Guest Pair with an Attomolar Dissociation Constant. *Angew. Chem. Int. Ed.* **2014**, *53*, 988-993.
25. Whitty, A., Cooperativity and Biological Complexity. *Nat. Chem. Biol.* **2008,** *4*, 435-439.
26. Rebek Jr, J., Simultaneous Encapsulation: Molecules Held at Close Range. *Angew. Chem. Int. Ed.* **2005,** *44*, 2068-2078.

27. Wang, K.; Jordan, J. H.; Hu, X.-Y.; Wang, L., Supramolecular Strategies for Controlling Reactivity within Confined Nanospaces. *Angew. Chem. Int. Ed.* **2020,** *59*, 13712-13721.
28. Klosterman, J. K.; Yamauchi, Y.; Fujita, M., Engineering Discrete Stacks of Aromatic Molecules. *Chem. Soc. Rev.* **2009,** *38*, 1714-1725.
29. Yoshizawa, M., Coordination Nanocages for Engineering Discrete Aromatic Stacks. In *Metal–Molecular Assembly for Functional Materials*, Matsuo, Y.; Higuchi, M.; Negishi, Y.; Yoshizawa, M.; Uemura, T.; Takaya, H.; Ueno, T.; Takeuchi, M.; Yoshimoto, S., Eds. Springer Japan: Tokyo, 2013; pp 29-39.
30. Rizzuto, F. J.; von Krbek, L. K. S.; Nitschke, J. R., Strategies for Binding Multiple Guests in Metal–Organic Cages. *Nat. Rev. Chem.* **2019,** *3*, 204-222.
31. Chen, X.-Y.; Mao, H.; Feng, Y.; Cai, K.; Shen, D.; Wu, H.; Zhang, L.; Zhao, X.; Chen, H.; Song, B.; Jiao, Y.; Wu, Y.; Stern, C. L.; Wasielewski, M. R.; Stoddart, J. F., Radically Enhanced Dual Recognition. *Angew. Chem. Int. Ed.* **2021,** *60*, 25454-25462.
32. Jiao, T.; Cai, K.; Liu, Z.; Wu, G.; Shen, L.; Cheng, C.; Feng, Y.; Stern, C. L.; Stoddart, J. F.; Li, H., Guest Recognition Enhanced by Lateral Interactions. *Chem. Sci.* **2019,** *10*, 5114-5123.
33. Ma, Y.-L.; Ke, H.; Valkonen, A.; Rissanen, K.; Jiang, W., Achieving Strong Positive Cooperativity through Activating Weak Non-Covalent Interactions. *Angew. Chem. Int. Ed.* **2018,** *57*, 709-713.
34. Sobiech, T. A.; Zhong, Y.; Sánchez B, L. S.; Kauffmann, B.; McGrath, J. K.; Scalzo, C.; Miller, D. P.; Huc, I.; Zurek, E.; Ferrand, Y.; Gong, B., Stable Pseudo[3]rotaxanes with Strong Positive Binding Cooperativity Based on Shape-Persistent Aromatic Oligoamide Macrocycles. *Chem. Commun.* **2021,** *57*, 11645-11648.
35. Sobiech, T. A.; Zhong, Y.; Miller, D. P.; McGrath, J. K.; Scalzo, C. T.; Redington, M. C.; Zurek, E.; Gong, B., Ultra-Tight Host–guest Binding with Exceptionally Strong Positive Cooperativity. *Angew. Chem. Int. Ed.* **2022,** *61*, e202213467.
36. Greenfield, J. L.; Wade, J.; Brandt, J. R.; Shi, X. Y.; Penfold, T. J., Fuchter, M. J., Pathways to Increase the Dissymmetry in the Interaction of Chiral Light and Chiral Molecules. *Chem. Sci.* **2021**, *12*, 8589-8602.
37. Inagaki, S.; Yamamura, K.; Nakasuji, K.; Nakazawa, T.; Murata, I., Charge-Transfer Transition for Symmetry-Forbidden Charge-Transfer Interaction in 1,4-dihydro-1,4-bis(dicyanomethylene)triptycenes. *J. Am. Chem. Soc.* **1981,** *103*, 2093-2094.
38. Weh, M.; Rühe, J.; Herbert, B.; Krause, A.-M.; Würthner, F., Deracemization of Carbohelicenes by a Chiral Perylene Bisimide Cyclophane Template Catalyst. *Angew. Chem. Int. Ed.* **2021,** *60*, 15323-15327.
39. Hibbert, D. B.; Thordarson, P., The Death of the Job Plot, Transparency, Open Science and Online Tools, Uncertainty Estimation Methods and Other Developments in Supramolecular Chemistry Data Analysis. *Chem. Commun.* **2016,** *52*, 12792-12805.
40. Zeng, F.; Cheng, L.; Ou, G.-C.; Tang, L.-L.; Ding, M.-H., Pyromellitic Diimide-Extended Pillar[6]arene: Synthesis, Structure, and Its Complexation with Polycyclic Aromatic Hydrocarbons. *J. Org. Chem.* **2022,** *87*, 3863-3867.
41. Chen, H.; Roy, I.; Myong, M. S.; Seale, J. S. W.; Cai, K.; Jiao, Y.; Liu, W.; Song, B.; Zhang, L.; Zhao, X.; Feng, Y.; Liu, F.; Young, R. M.; Wasielewski, M. R.; Stoddart, J. F., Triplet–Triplet Annihilation Upconversion in a Porphyrinic Molecular Container. *J. Am. Chem. Soc.* **2023,** *145*, 10061-10070.
42. Nishio, M.; Umezawa, Y.; Honda, K.; Tsuboyama, S.; Suezawa, H., CH/π Hydrogen Bonds in Organic and Organometallic chemistry. *CrystEngComm* **2009,** *11*, 1757-1788.
43. Spackman, M. A.; Jayatilaka, D., Hirshfeld Surface Analysis. *CrystEngComm* **2009,** *11*, 19-32.
44. Riehl, J. P.; Richardson, F. S., Circularly Polarized Luminescence Spectroscopy. *Chem. Rev.* **1986,** *86*, 1-16.
45. Sánchez-Carnerero, E. M.; Agarrabeitia, A. R.; Moreno, F.; Maroto, B. L.; Muller, G.; Ortiz, M. J.; de la Moya, S., Circularly Polarized Luminescence from Simple Organic Molecules. *Chem. Eur. J.* **2015,** *21*, 13488-13500.
46. Kumar, J.; Nakashima, T.; Kawai, T., Circularly Polarized Luminescence in Chiral Molecules and Supramolecular Assemblies. *J. Phys. Chem. Lett.* **2015,** *6*, 3445-3452.
47. Nizar, N. S. S.; Sujith, M.; Swathi, K.; Sissa, C.; Painelli, A.; Thomas, K. G., Emergent Chiroptical Properties in Supramolecular and Plasmonic Assemblies. *Chem. Soc. Rev.* **2021**, *50*, 11208-11226.
48. Yeom, J.; Santos, U. S.; Chekini, M.; Cha, M.; de Moura, A. F.; Kotov, N. A., Chiromagnetic Nanoparticles and Gels. *Science* **2018,** *359*, 309-314.
49. Han, J.; Yang, D.; Jin, X.; Jiang, Y.; Liu, M.; Duan, P., Enhanced Circularly Polarized Luminescence in Emissive Charge-Transfer Complexes. *Angew. Chem. Int. Ed.* **2019,** *58*, 7013-7019.
50. Gu, Q.; Chen, Z.; Xie, W.; Qiu, W.; Peng, X.; Jiao, Y.; Li, M.; Liu, Z.; Sun, G.; Lu, Y.; Gan, Y.; Liu, K.; Zhao, Z.; Su, S.-J., Chiral Exciplex Acceptor Enables Circularly Polarized Electroluminescence with High Dissymmetry Factor Close to 10^{-2}. *Adv. Opt. Mater.* **2022,** *10*, 2201793.
51. Chen, Z.; Huang, M.; Zhong, C.; Cao, X.; Xie, G.; Gong, S.; Yang, C., Cascade Chirality Transfer Through Diastereomeric Interaction Enables Efficient Circularly Polarized Electroluminescence. *Adv. Funct. Mater.* **2023,** *33*, 2215179.
52. Adelizzi, B.; Chidchob, P.; Tanaka, N.; Lamers, B. A. G.; Meskers, S. C. J.; Ogi, S.; Palmans, A. R. A.; Yamaguchi, S.; Meijer, E. W., Long-Lived Charge-Transfer State from B–N Frustrated Lewis Pairs Enchained in Supramolecular Copolymers. *J. Am. Chem. Soc.* **2020,** *142*, 16681-16689.
53. An, S.; Hao, A.; Xing, P., Polyhedral Oligosilsesquioxanes in Functional Chiral Nanoassemblies. *Angew. Chem. Int. Ed.* **2021,** *60*, 9902-9912.
54. Zhang, Y.; Yu, W.; Li, H.; Zheng, W.; Cheng, Y., Induced CPL-Active Materials Based on Chiral Supramolecular Co-Assemblies. *Chem. Eur. J.* **2023,** *29*, e202204039.
55. Sang, Y.; Han, J.; Zhao, T.; Duan, P.; Liu, M., Circularly Polarized Luminescence in Nanoassemblies: Generation, Amplification, and Application. *Adv. Mater.* **2020,** *32*, 1900110.
56. Zhao, T.; Han, J.; Duan, P.; Liu, M., New Perspectives to Trigger and Modulate Circularly Polarized Luminescence of Complex and Aggregated Systems: Energy Transfer, Photon Upconversion, Charge Transfer, and Organic Radical. *Acc. Chem. Res.* **2020,** *53*, 1279-1292.
57. Chen, J.-F.; Gao, Q.-X.; Liu, L.; Chen, P.; Wei, T.-B., A Pillar[5]arene-Based Planar Chiral Charge-Transfer Dye with Enhanced Circularly Polarized Luminescence and Multiple Responsive Chiroptical Changes. *Chem. Sci.* **2023,** *14*, 987-993.
58. Zhang, D.-W.; Li, M.; Chen, C-F., Recent Advances in Circularly Polarized Electroluminescence Based on Organic Light-Emitting Diodes. *Chem. Soc. Rev.* **2020**, *49*, 1331-1343.
59. Ottolenghi, M., Charge-Transfer Complexes in the Excited State. Laser Photolysis Studies. *Acc. Chem. Res.* **1973,** *6*, 153-160.

TOC Graphics